

Article

# Tracing the Relationship between Precipitation and River Water in the Northern Carpathians Base on the Evaluation of Water Isotope Data

Viorica Nagavciuc <sup>1,2,3,\*</sup> , Carmen-Andreea Bădăluță <sup>2,3,4</sup> and Monica Ionita <sup>5</sup><sup>1</sup> Faculty of Forestry, Ștefan cel Mare University of Suceava, 720229 Suceava, Romania<sup>2</sup> Institute for Geological and Geochemical Research, Research Centre for Astronomy and Earth Sciences, Hungarian Academy of Sciences, 1112 Budapest, Hungary; carmenbadaluta@yahoo.com<sup>3</sup> Stable Isotope Laboratory, Ștefan cel Mare University of Suceava, 720229 Suceava, Romania<sup>4</sup> Department of Geography, Ștefan cel Mare University of Suceava, 720229 Suceava, Romania<sup>5</sup> Paleoclimate Dynamics Group, Alfred-Wegener-Institute for Polar and Marine Research, Bussestrasse 24, D-27570 Bremerhaven, Germany; Monica.Ionita@awi.de

\* Correspondence: nagavciuc.viorica@gmail.com; Tel.: +40-751-966-785

Received: 18 January 2019; Accepted: 28 April 2019; Published: 2 May 2019



**Abstract:** The aim of this study is to investigate the stable isotope composition of precipitation and river water from the northeastern part of Romania. For this study, we collected monthly samples (for variable periods of time) of precipitation from six stations, and river water from three stations, between March 2012 and December 2017. The precipitation in the area is sourced mainly from the Atlantic Ocean, and secondarily from the Black Sea, local recycling being important especially in summer. We found that the seasonal  $\delta^{18}\text{O}$  in precipitation is in agreement with the seasonal temperature variability, as shown by the significant correlation coefficient between the two variables ( $r = 0.77$ ), which indicates that the temperature has an important role in the  $\delta^{18}\text{O}$  variability in precipitation water in this region. The local meteoric water line in the northeastern part of Romania is defined by the equation  $\delta^2\text{H} = 7.80 \times \delta^{18}\text{O} + 7.47$ , ( $r^2 = 0.99$ ,  $n = 121$ ). The results presented in this study emphasize that the  $\delta^{18}\text{O}$  (and  $\delta^2\text{H}$ ) and d-excess variability are strongly influenced by temperature, precipitation and the prevailing large-scale atmospheric circulation.

**Keywords:** stable isotopes; oxygen; hydrogen; precipitation; river; deuterium excess; Romania

## 1. Introduction

The stable oxygen and hydrogen isotope composition of precipitation and/or river water exhibit large spatial and temporal variation across the Earth's surface [1], thus being useful tracers of the processes in the water cycle, being linked to air moisture sources. Also, they contribute to advancing the understanding of the atmospheric hydrological cycle, which is related to climate and linkages between precipitation surface and groundwater flow [2–5]. The stable isotopes of oxygen and hydrogen in precipitation also reflect the combination of source-region rainout effects and recycling effects which are affected by air masses bringing water vapor from different geographic regions [1]. As a result, they offer the possibility to identify the sources of precipitation and quantify the contribution of regional and local sources to the runoff generation [6,7], as well as the dynamics of catchment-specific processes (e.g., evaporation, mixing different sources) [8]. Variation of the  $\delta^{18}\text{O}$  and  $\delta^2\text{H}$  in precipitation water is a function of conditions at the moisture source(s), processes along the path to the precipitation site and site-specific conditions during precipitation [7,9,10]. An important role is played by the large-scale atmospheric circulation, which leads to changes in the moisture sources and the conditions during transport and precipitation [6,9,11,12]. Detailed analyses of the relationship between stable isotopes in

precipitation and river water could give further information on regional and global scale hydrological processes, thus enabling better planning for water usage in the context of future potential changes in the climate system [12].

In order to better understand the dynamics of water in a given watershed using the stable isotopes of oxygen and hydrogen, a two-step approach is required: First, identification of the contribution of regional and local moisture sources to precipitation generation, and second, identification of links between stable isotopic composition and atmospheric and hydrologic processes affecting surface water [13].

A remarkable number of studies which investigate the relationship between hydrogen and oxygen isotopes in precipitation and river water have been carried out in Europe [3,13–17], and elsewhere in the world [2,4,12,18–20], but currently, similar studies in the Eastern Carpathian Mountains, the main recharge area for rivers in Southeast Europe, are missing. To fill this gap in knowledge, we have designed a study aiming: i) To investigate the temporal and spatial variations of the stable isotope compositions of precipitation and river water from the northeastern part of Romania, in order to identify the impact of different local, regional and large-scale factors on the variability of oxygen and hydrogen isotopic composition using the available isotopic data set; ii) to define the local meteoric water line (LMWL) over the analyzed region; and iii) to investigate the relation between air moisture sources and the prevailing large-scale atmospheric circulation. In this study we provide the preliminary database of the oxygen and hydrogen isotopes in precipitation and river from the northeastern part of Romania which will improve our understanding regarding the temporal and spatial variations of the stable isotopic compositions in precipitation and river water. These could further provide information on regional and global scale hydrological processes, enabling a better planning of water usage in the context of future climatic changes [12].

## 2. Materials and Methods

### 2.1. Study Site

The study area was located in the northeastern part of Romania, along a west–east transect through the Eastern Carpathian Mountains (Figure 1), including the low-lying Bistrița-Năsăud station (BN, 380 m above sea level) on the western slope of the Carpathian Mountains, the high-elevation Rarău (RA, 1600 m) and Gura Haiti (GH, 1200 m) stations, the intra-mountain Vatra Dornei (VD, 800 m) and Câmpulung Moldovenesc (CM, 700 m) stations and the low-lying Suceava station (350 m) on the eastern slopes of the Carpathian Mountains (Figure 2).

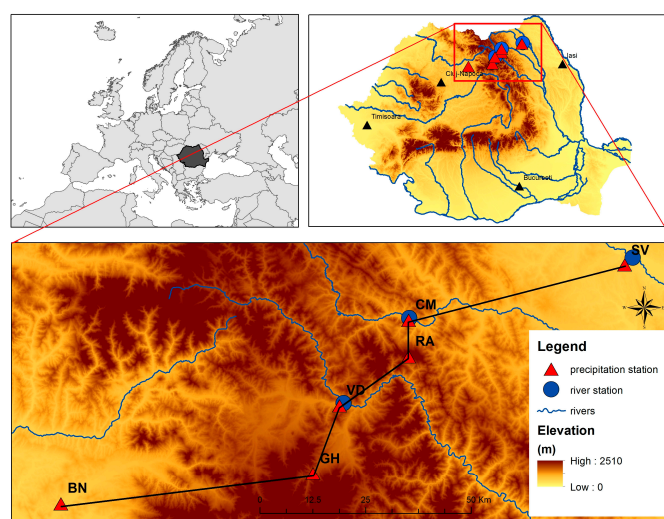


**Figure 1.** Site location in Europe (top left), in Romania (top right) and in the local context (bottom): Bistrița-Năsăud (BN), Gura Haiti (GH), Vatra Dornei (VD), Rarău (RA), Câmpulung Moldovenesc (CM) and Suceava (SV). The black line represents the position of the elevation profile from Figure 2.

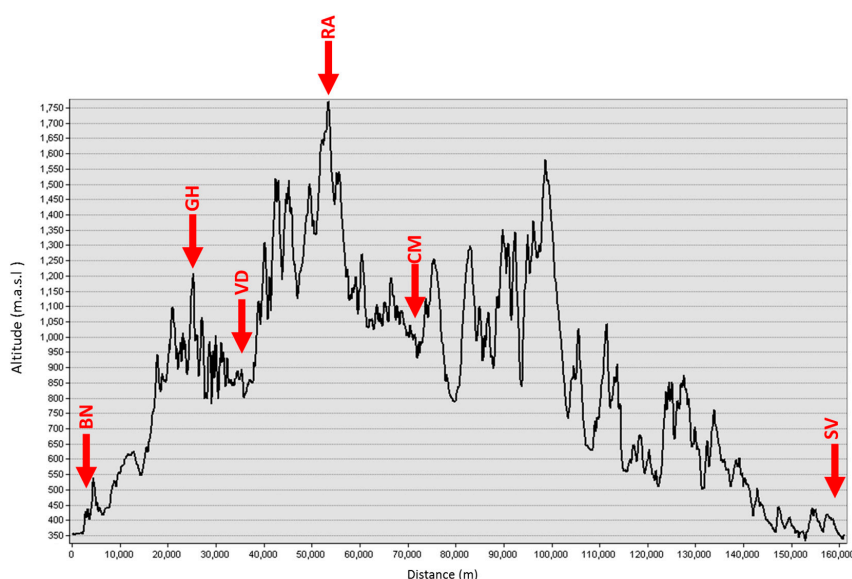


**Figure 2.** The west–east elevation profile of the study site, the black line from Figure 1, Bistrița-Năsăud (BN), Gura Haiti (GH), Vatra Dornei (VD), Rarău (RA), Câmpulung Moldovenesc (CM) and Suceava (SV).

The local climate is temperate continental [21]. The mean annual temperature and precipitation amount, based on the gridded E-OBS data set (daily gridded observational dataset), with resolution of  $0.25^\circ \times 0.25^\circ$  [22] for the 1961–1990 are as follows: 8.1 °C and 686 mm/year at Bistrița-Năsăud, 2.3 °C and 954 mm/year at Rarău, and 7.6 °C and 603 mm/year at Suceava.

## 2.2. Samples Collection and Stable Isotope Measurements

For this study, monthly rainwater samples were collected at six locations and river water at three locations as described (Table 1).

**Table 1.** The name of the precipitation and rivers of the study sites, with corresponding abbreviation, coordinates, elevation, study period and number of samples for each site.

Nr.	Station Name	Abbreviation	Latitude	Longitude	Elevation (m.a.s.l.)	Sampling Period	Number of Samples
1	Bistrița-Năsăud	BN	47°7' N	24°29' E	380	March 2012–January 2014 and January 2015–November 2015	45
2	Gura Haiti	GH	47°11' N	25°16' E	1200	October 2014–July 2015	8
3	Vatra Dornei	VD	47°20' N	25°21' E	800	October 2014–July 2015	7
4	Rarău	RA	47°27' N	25°34' E	1600	May 2013–January 2017	27
5	Câmpulung Moldovenesc	CM	47°31' N	25°34' E	700	October 2014–February 2016	12
6	Suceava	SV	47°37' N	26°14' E	350	December 2012–November 2017	49
7	Suceava River	SVr	47°39' N	26°15' E	275	July 2014–March 2017	33
8	Bistrița River	BNr	47° 7' N	24°29' E	340	December 2014–March 2017	24
9	Moldova River	Mr	47°31' N	25°34' E	660	October 2014–February 2016	14

Sampling was done according to the specifications of the International Atomic Energy Agency by using 5 L HDPE (high density polyethylene) collectors. For precipitation, we collected an aliquot at the end of each month, while grab samples were collected for rivers on the last day ( $\pm 1$  day) of each month. River water samples were collected in the vicinity of the precipitation stations (Suceava River (SVr), Bistrița River (BNr) and Moldova River (Mr), Table 1 and Figure 1). At the end of each month, a sample was taken directly from 30 to 40 cm below the surface of water in the main stream of the rivers. River water samples were stored and analyzed similar to precipitation ones. Full details of the sampling procedure are given in [23].

Samples were analyzed for their stable isotopic composition at the Stable Isotope Laboratory, Ștefan cel Mare University of Suceava, in Suceava, Romania, using a Picarro L2130i CRDS analyzer

coupled to a high precision vaporizing module. Prior to analyses, all samples were filtered through a 0.45  $\mu\text{m}$  nylon membrane. Each sample was manually injected in the vaporization at least six times until the standard deviation of the last four injections was less than 0.05 for  $\delta^{18}\text{O}$  and 0.5 for  $\delta^2\text{H}$ , respectively. The average of these last four injections was used as the accepted value, further normalized using two internal standards calibrated against Vienna Standard Mean Ocean Water 2 (VSMOW2) and Standard Light Antarctic Precipitation 2 (SLAP2) standards provided by the International Atomic Energy Agency (IAEA). A third standard was used to check the long-term stability of the analyzer. The stable isotope composition of oxygen and hydrogen is reported using standard  $\delta$  notation:

$$\delta = ((R_x - R_{\text{std}})/R_{\text{std}}) \times 1000, \quad (1)$$

where,  $\delta$  represent  $\delta^{18}\text{O}$  or  $\delta^2\text{H}$  value,  $R_x$  and  $R_{\text{std}}$  are  $^{18}\text{O}/^{16}\text{O}$  and  $^2\text{H}/^1\text{H}$  ratios of the sample (x) and the standard (std), respectively. The precision is estimated to be better than 0.16‰ for  $\delta^{18}\text{O}$  and 0.7‰ for  $\delta^2\text{H}$ , respectively, based on repeated measurements of an internal standard.

The d-excess parameter (d), expressed as  $d = \delta^2\text{H} - 8 \times \delta^{18}\text{O}$  [24], was calculated for precipitation samples in order to obtain additional information on air moisture source conditions and thus track changes of air moisture source and atmospheric circulation patterns [25].

LMWL was calculated using the ordinary least squares regression (OLSR) model, which in its form of  $y = a \times x + b$ , gives the same weighting to all isotopic data regardless of the monthly precipitation amount they represent [26,27].

### 2.3. Climate Data

For the analysis of climate-stable isotope composition relationship, we used the monthly mean air temperature and precipitation amount data of the nearest grid point to our sampling station from the gridded E-OBS [22], for the 2012–2017 period. To investigate the large-scale atmospheric circulation in relationship with the stable isotope composition of precipitation, we used the monthly means of geopotential height at 500 millibars (mb) (Z500), zonal wind (U500) and meridional wind (V500) at 500 mb provided by the National Center for Atmospheric Research (NCAR) [26]. The snow cover data was provided by MODIS/Terra Snow Cover Monthly L3 Global 0.05Deg CMG, Version 6 [27].

## 3. Results and Discussion

### 3.1. Basic Characteristics of $\delta^2\text{H}$ and $\delta^{18}\text{O}$ in Precipitation and River Water

The maximum  $\delta$  values were registered at the low elevation SV and BN stations, and the minimum ones at the high elevation stations RA, CM, GH, and VD (Figure 3, Table 2). The low  $\delta^2\text{H}$  and  $\delta^{18}\text{O}$  values registered at VD were the result of the station's location in an intra-montane depression, with strong thermal inversions in winter. Except for VD and GH stations (which had only several months-long sampling periods), a good inverse correlation was seen between  $\delta$  values and elevation. The average  $\delta^{18}\text{O}$  lapse rate was 0.25‰/100 m for the BN (380 m asl) – RA (1600 m asl) transect (western slope of the Carpathians) and 0.27‰/100 m for the SV (350 m asl) – RA (1600 m asl) transect (eastern slope of the Carpathians). Similar results have been found for the eastern Carpathian transect (0.27‰/100 m) [23] and close value have been reported for the western Carpathian in Slovakia (0.21‰/100 m) [28]. Because of the short time series at the GH, CM and VD stations, data from these stations was discussed together with that from RA.

For the river water the highest values were registered at SVr station and the lowest ones at Mr station (Table 3), following a similar path as the one of the precipitation: Decreasing values with increasing elevation.

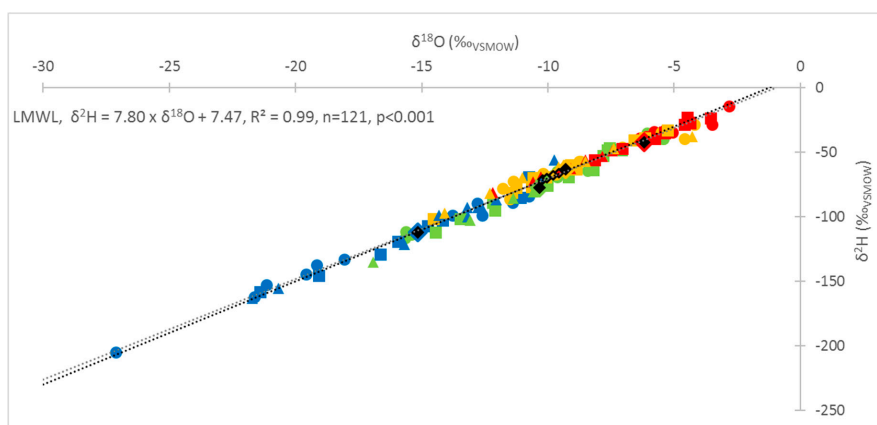


**Figure 3.** The stable isotope composition of precipitation water from SV (circle), BN (square) and RA (triangle) for winter (blue) spring (green), summer (red) and autumn (orange). The mean values for each season are represent by rhomb with black contour marks for river water, and with rhomb with black full marks for precipitation. The dotted black line represents the GMWL (Global Meteoric Water Line) and the dotted gray line represents local meteoric water line (LMWL).

**Table 2.** The mean, maximum (max), and minimum (min)  $\delta^{18}\text{O}$  and  $\delta^2\text{H}$  values in precipitation water at Câmpulung Moldovenesc (GM), Vatra Dornei (VD), Gura Haiti (GH), Rarău (RA), Suceava (SV) and Bistrița-Năsăud (BN) stations.

	CM		VD		GH		RA		SV		BN	
	$\delta^{18}\text{O}$	$\delta^2\text{H}$										
<b>Mean</b>	-11.1	-85	-12.1	-89	-11.4	-85	-11.6	-82	-9.9	-71	-9.7	-69
<b>Max</b>	-5.7	-37	-7.0	-45	-6.8	-43	-4.3	-33	1.1	-2	-3.5	-23
<b>Min</b>	-18.7	-151	-16.7	-129	-15.7	-121	-21.7	-163	-27.1	-205	-21.4	-158

**Table 3.** The mean, maximum (max), and minimum (min)  $\delta^{18}\text{O}$  and  $\delta^2\text{H}$  values in river water at Suceava (SVr), Moldova (Mr) and Bistrita (BNr) river stations.

	SVr		Mr		BNr	
	$\delta^{18}\text{O}$	$\delta^2\text{H}$	$\delta^{18}\text{O}$	$\delta^2\text{H}$	$\delta^{18}\text{O}$	$\delta^2\text{H}$
<b>mean</b>	-9.6	-67.4	-10.1	-70.8	-9.9	-68.4
<b>min</b>	-10.8	-74.6	-10.6	-74.2	-10.5	-72.1
<b>max</b>	-8.8	-62.7	-9.5	-66.1	-8.9	-64.6

The highest values of both  $\delta^{18}\text{O}$  and  $\delta^2\text{H}$  occurred during the summer period (June, July and August). They decreased during the autumn season (September, October and November) and reached a minimum throughout the winter months (December, January and February). The seasonal distribution of the stable isotope composition of river waters allows for the delineation of two periods: A winter–spring period (from December to May) and a summer–autumn period (from June until November) (Figure 4). In the winter–spring period, the mean values were  $-10.0\text{‰}$  for  $\delta^{18}\text{O}$  and  $-70\text{‰}$  for  $\delta^2\text{H}$  at SVr,  $-10.4\text{‰}$  for  $\delta^{18}\text{O}$  and  $-73\text{‰}$  for  $\delta^2\text{H}$  at Mr and  $-10.0\text{‰}$  for  $\delta^{18}\text{O}$  and  $-69\text{‰}$  for  $\delta^2\text{H}$  at BNr. For the summer–autumn period, the mean values were  $-9.3\text{‰}$  for  $\delta^{18}\text{O}$  and  $-65\text{‰}$  for  $\delta^2\text{H}$  at SVr,  $-9.8\text{‰}$  for  $\delta^{18}\text{O}$  and  $-69\text{‰}$  for  $\delta^2\text{H}$  at Mr and  $-9.9\text{‰}$  for  $\delta^{18}\text{O}$  and  $-68\text{‰}$  for  $\delta^2\text{H}$  at BNr.

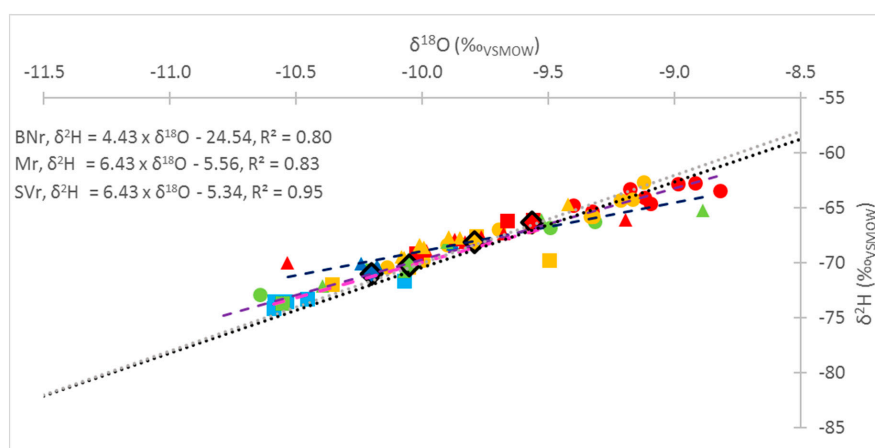


**Figure 4.** The stable isotope composition of river water from SVr (circle) BNr (square) and Mr (triangle) for winter (blue) spring (green), summer (red) and autumn (orange). The mean values for each season are represented by rhomboids with black contour marks. The dotted black line represents the GMWL and the dotted gray line represents LMWL.

The amplitude for the river isotopic composition ranged between 1.1‰ and 2‰ for  $\delta^{18}\text{O}$ , and between 7‰ and 12‰ for  $\delta^2\text{H}$ , while for the precipitation water, the amplitude ranged between 17‰ and 28‰ for  $\delta^{18}\text{O}$ , and 126‰ and 202‰ for  $\delta^2\text{H}$ . The small amplitude of stable isotope values in river waters and a little more negative compared to precipitation in winter and spring time reveal that the river basins have a significant sub-surface water storage capacity, while the snowmelt water or/and precipitation water contribute in a smaller proportion to the total river water flow [7].

### 3.2. Local Meteoric Water Line

To define the local meteoric line (LMWL) in the northeastern part of Romania, all samples from the study site were used, and the relationship was established as:

$$\delta^2\text{H} = 7.61 \times \delta^{18}\text{O} + 3.93 \quad (r^2 = 0.96, n = 154, p < 0.001). \quad (2)$$

However, this LMWL considered all samples, including those from VD, CM and GH stations that only cover the cold half year. When only the three stations for which data from all seasons is available, the LMWL is defined by the equation:

$$\delta^2\text{H} = 7.52 \times \delta^{18}\text{O} + 3.83 \quad (r^2 = 0.96, n = 120, p < 0.001). \quad (3)$$

Both the slope and the intercept were lower than the corresponding values of the GMWL (Global Meteoric Water Line), which could result partly from sub-cloud evaporation of the falling raindrops through dry air during summer [4]. When samples that show clear signs of evaporative enrichment (either in the atmosphere or during collection) were removed, the LMWL is defined by the equation:

$$\delta^2\text{H} = 7.80 \times \delta^{18}\text{O} + 7.47 \quad (r^2 = 0.99, n = 121, p < 0.001). \quad (4)$$

Interestingly, the three equations above suggest that adding data from the cold season (November through April) does not change the characteristics of the LMWLs. We have further tested this assumption by constructing LMWLs for winter (W-LMWL) and summer (S-LMWL) only. The results show that stations at similar elevation had W-LMWL with similar characteristics (slope and intercept), but with increasing slope with elevation, being closer to the GMLW at the highest stations (RA). S-LMWLs had lower slopes and similarly variable intercept values, likely reflecting a higher contribution from local, re-evaporated, moisture sources and sub-cloud evaporation after precipitation during summer [29].

These differences likely reflect the high evaporative conditions during summer in the low lying Pannonian Plain (Debrecen) and Eastern Ukrainian Plain (Kharkiv) compared to our study region. Intermediary values between Pannonian Plain and Eastern Ukrainian were found at Dumbrava station in southwestern Romania, where the LMWL has intermediate characteristics [30] being defined by the equation.

Separately for the stations for which a full year was covered, the LMWLs were as follows:

$$\text{SV} \quad \delta^2\text{H} = 7.70 \times \delta^{18}\text{O} + 6.54 \quad (r^2 = 0.99, n = 48, p < 0.001), \quad (5)$$

$$\text{BN} \quad \delta^2\text{H} = 7.98 \times \delta^{18}\text{O} + 8.77 \quad (r^2 = 0.99, n = 44, p < 0.001), \quad (6)$$

$$\text{RA} \quad \delta^2\text{H} = 8.30 \times \delta^{18}\text{O} + 14.70 \quad (r^2 = 0.98, n = 26, p < 0.001), \quad (7)$$

All slopes were close to the GMWL, whereas the slightly lower intercepts at SV and BN (low elevation stations) might reflect evaporative loss into the unsaturated air during summer precipitation events [6,31]. Contrary, the LMWL at the high-elevation RA site potentially reflects the high overall relative humidity during precipitation events [3,32].

### 3.3. Stable Isotopes in Precipitations–Climate Relationship

The  $\delta^{18}\text{O}$  values in precipitation showed high correlation coefficients with the mean air temperature ( $r = 0.85$  at BN,  $r = 0.73$  at RA and  $r = 0.75$  at SV) (Figures 5 and 6) and low correlation coefficients with the precipitation ( $r = 0.35$  at BN,  $r = 0.23$  at RA and  $r = 0.39$  at SV). The strong correlation between  $\delta^{18}\text{O}$  in precipitation at all three stations and the mean air temperature indicated that the temperature has an important role in  $\delta^{18}\text{O}$  variability in precipitation water in this region (Figure 6). The monthly variations of  $\delta^{18}\text{O}$  and  $\delta^2\text{H}$  in precipitation showed a clear seasonal cycle, with the highest  $\delta^{18}\text{O}$  and  $\delta^2\text{H}$  values in summer (June to August) and the lowest values registered in winter (December to February) (Figure 5). Significant correlations between water isotopes in precipitation and monthly mean air temperature were also found in other studies in Romania [33–35]. The seasonal changes of the  $\delta^{18}\text{O}$  and  $\delta^2\text{H}$  in precipitation mirrored the seasonal changes in the mean air temperature. The  $\delta^{18}\text{O}$  and  $\delta^2\text{H}$  in precipitation were affected by the changes of the stable isotope composition of the water vapor in the atmosphere, which were influenced by the seasonal variation of evapotranspiration fluxes over the continents and by the seasonal variation of large-scale atmospheric circulation patterns which influence the origin of air moisture sources [24,36].

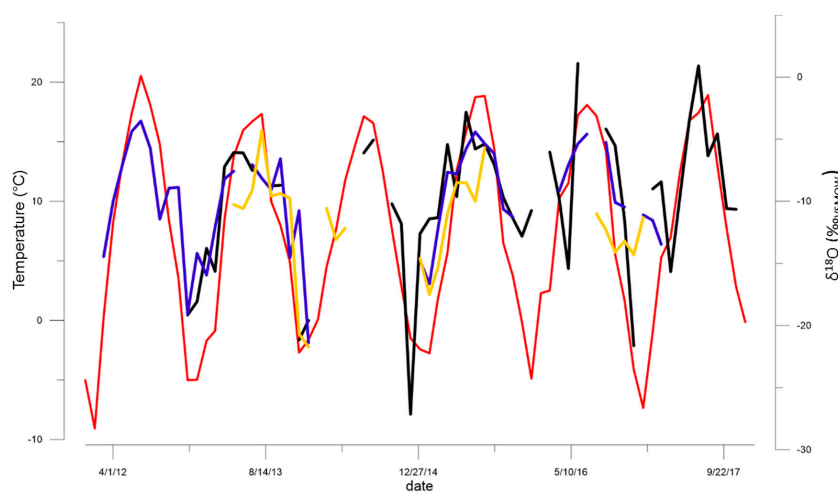


**Figure 5.** Monthly variation of mean temperature (red) from the gridded E-OBS (daily gridded observational dataset) of the nearest point of the stations and  $\delta^{18}\text{O}$  in precipitation at BN (blue), SV (black) and RA (yellow).

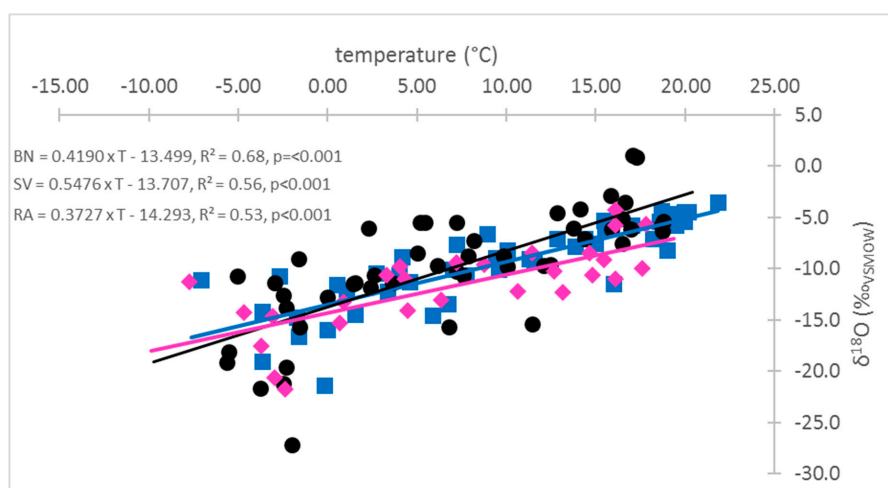


**Figure 6.** Correlation between mean temperature and  $\delta^{18}\text{O}$  in precipitation at BN (square blue), SV (circle black) and RA (rhomb magenta).

The weak relationship between  $\delta^{18}\text{O}$  (and  $\delta^2\text{H}$ ) in precipitation and precipitation amount indicated that the rainfall amount did not have a strong influence over the  $\delta^{18}\text{O}$  (and  $\delta^2\text{H}$ ) variability over the study region [7,37].

#### 3.4. Deuterium Excess (d-) in Precipitation and Large-scale Atmospheric Circulation

For the analyzed period, the d-excess in precipitation samples varied widely, between  $-4\text{‰}$  (August 2013) and  $22\text{‰}$  (November 2013) at RA, between  $-21\text{‰}$  (March 2016) and  $18\text{‰}$  (November 2015) at SV, and between  $-24\text{‰}$  (June 2015) and  $17\text{‰}$  (December 2013) at BN. Low values ( $< 3\text{‰}$ ) were generally recorded during summer months, and high ( $> 15\text{‰}$ ) during late autumn and winter. In the transition seasons (spring and autumn) the d-excess values were close to the global average of  $10\text{‰}$ . Such distinct seasonal d-excess variability can be explained by the different sources of air moisture that reached the study area. In winter, the high d-excess values reflect the influence of the long-lived, mobile and intense Mediterranean cyclones [38], which are characterized by high d-excess values [39]. In summer, the low d-excess values reflect the hot and dry characteristic of the prevailing air masses, which encourage secondary evaporation processes after precipitation [40]. During several months, very low monthly d-excess values were registered (between  $-9\text{‰}$  and  $-24\text{‰}$ ). These low values occurred sporadically, in months with either 1) low precipitation amounts or 2) high temperatures. One such event occurred in June 2015, when at BN the d-excess was  $-24\text{‰}$ , while at SV and RA it was  $8.1\text{‰}$  and  $9\text{‰}$ , respectively.  $\delta^{18}\text{O}$  values in precipitation in June 2015 were  $-5.8\text{‰}$  at BN,  $-2.8\text{‰}$  at SV and  $-8.5\text{‰}$  at RA, following air temperatures values. A similar event was recorded also in June 2016, when at SV the d-excess was very low ( $-19.1\text{‰}$ ), while close to normal values were observed at RA ( $9.1\text{‰}$ ) and SV ( $8.1\text{‰}$ ). In the same time,  $\delta^{18}\text{O}$  in precipitation was  $+1.1\text{‰}$  at SV,  $-5.8\text{‰}$  at RA and  $-5.4\text{‰}$  at BN, respectively. In both these periods, high pressure systems were located over the eastern part of Europe and the combination of high temperatures and low precipitation amounts led to locally important deviations from the "normal" values of d-excess, likely triggered by sub-cloud and/or post-deposition evaporation. However, given the local nature of these "deviations" it is difficult to link d-excess variability to large-scale circulation patterns during summer. Contrary, the regional patterns of d-excess and  $\delta^{18}\text{O}$  variability in precipitation in snow allows for such putative linkages.

Thus, in December 2012, d-excess values were high ( $15.9\text{‰}$ ) at SV (eastern slopes of the Carpathians) and low ( $7.2\text{‰}$ ) at BN (western slopes of the Carpathians), while  $\delta^{18}\text{O}$  in precipitation was similar at the two stations ( $-19.1\text{‰}$ ). Given that climatic conditions were similar at the two stations, we excluded post-depositional alteration of the original d-excess values due to kinetic fractionation during snow sublimation. The low  $\delta^{18}\text{O}$  values would suggest a regionally important atmospheric circulation (likely

bringing cold air from N Europe), but the widely different d-excess values suggest different conditions at the moisture sources and thus possibly different moisture sources. In December 2012, a low-pressure system was prevailing over Europe, allowing for a northward intrusion of Mediterranean cyclones (Figure 7). These cyclones carried moisture from the highly evaporative eastern Mediterranean Sea, thus with a very high d-excess values. This moisture was discharged at contact with the northern cold air, thus resulting in the low  $\delta^{18}\text{O}$  and high d-excess at SV. Contrary, on the western slopes of the Carpathians (at BN) precipitation was delivered by eastward travelling winds originating in the Atlantic, imprinted with d-excess values close to the mean value in the region (10‰). Thus, a combination of large-scale circulation patterns with cold air dominating over the entire region (Figure 8) and the orographic barrier of the Carpathians resulted in this particular distribution of stable isotopes in precipitation in two close stations.

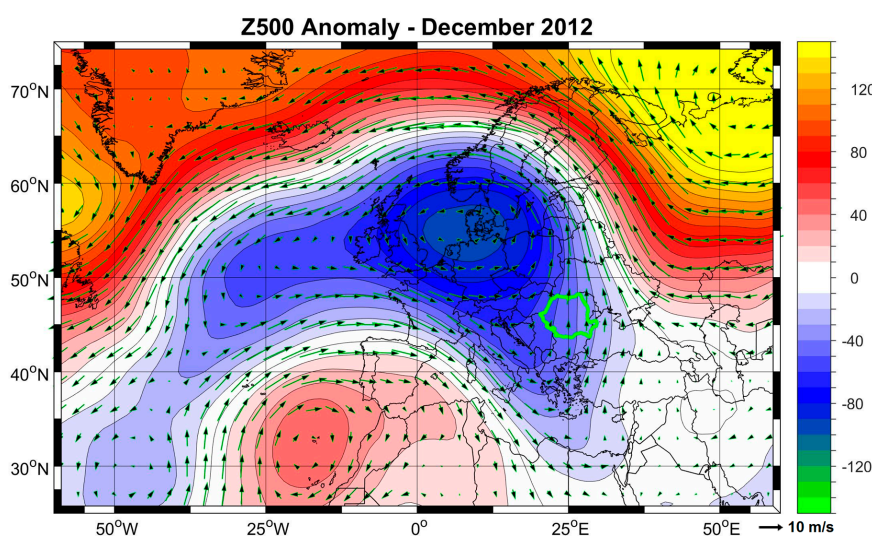


**Figure 7.** Geopotential height anomalies at 500 mb level (Z500) the events in December 2012.

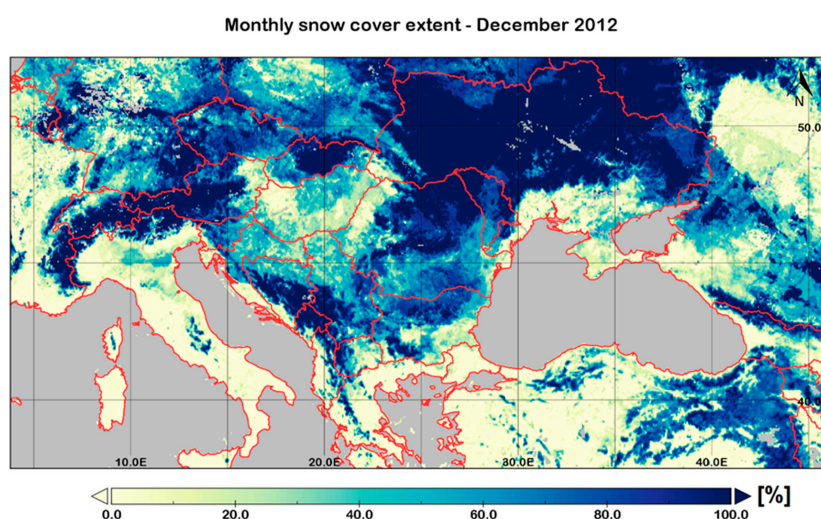


**Figure 8.** Large scale snow cover in December 2012. The snow cover data was provided by MODIS/Terra Snow Cover.

Contrary, in February 2015 d-excess values were lower than the global mean, but similar at all three station (2.1‰ at SV, 4.2‰ at RA and 0‰ at BN), while  $\delta^{18}\text{O}$  values were  $-14.4\text{‰}$  at SV,  $-17.5\text{‰}$  at RA and  $-16.3\text{‰}$  at BN. In February 2015, a high-pressure system was prevailing over northeastern

Romania. The anticyclonic circulation was accompanied by strong easterly winds advecting dry and cold air from continental Eastern Europe, resulting in the low  $\delta^{18}\text{O}$  and d-excess values (Figure 9a,b).

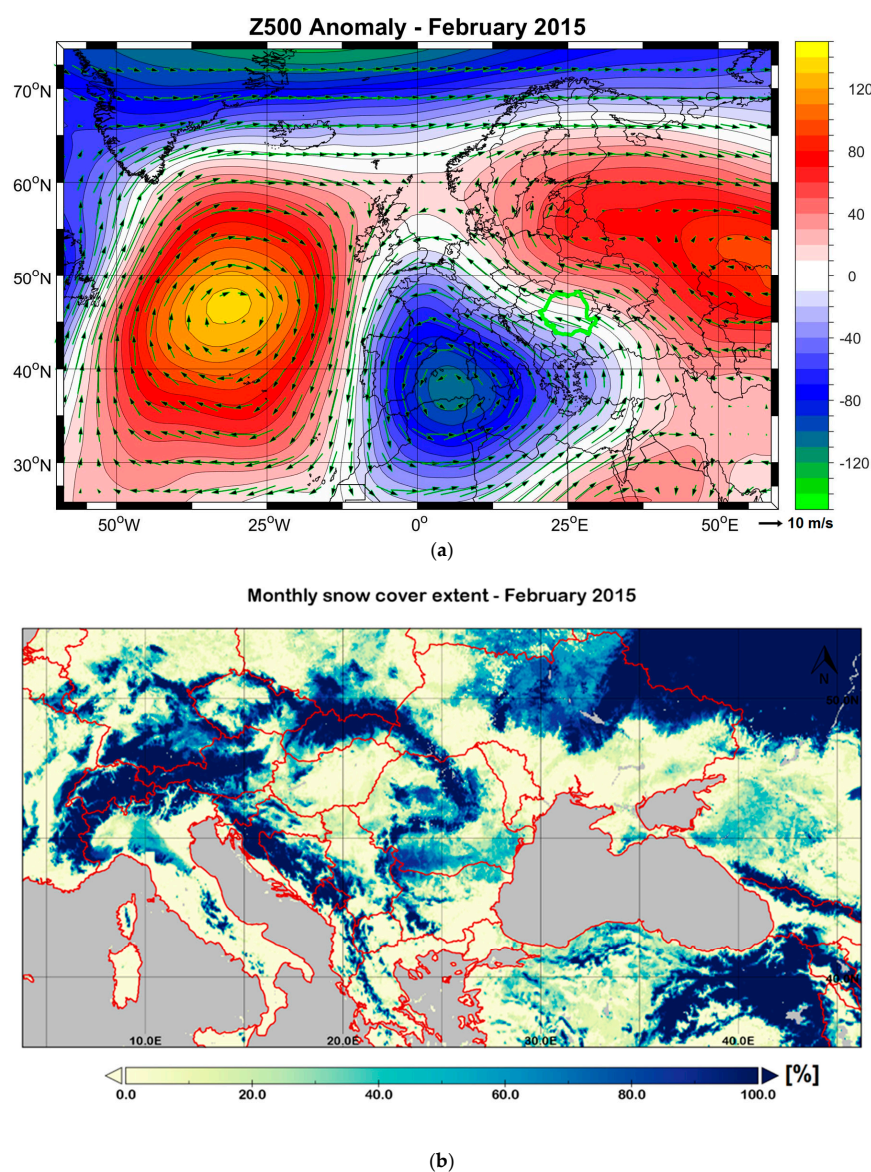


**Figure 9.** (a) Geopotential height anomalies at 500mb level (Z500) in February 2015; (b) large scale snow cover in February 2015. The snow cover data was provided by MODIS/Terra Snow Cover. Units: Z500(m).

Combined, the d-excess and  $\delta$  values suggest that, similar to southwestern and western Romania [33,41], Mediterranean cyclones have a strong imprint on winter precipitation in eastern Romania. Similar influences have been found also further to the east [42], showing that moisture originating from the Mediterranean and Black Seas reaches into the central East European plain.

### 3.5. Precipitation-River Relationships

The rivers analyzed in this study belong to a group, with minimum  $\delta$  values recorded in the winter time and low seasonal amplitudes in the  $\delta^{18}\text{O}$  [43]. Reduced amplitudes of stable isotope values in river water compared to precipitation water variability suggest that rivers are recharged via subsurface flow, with water from individual rain events being stored in the phreatic zone before recharging the rivers [17,43]. Low d-excess in river water occurs in summer, suggesting that evaporative loss

plays an important role in the hydrological balance in the region [23]. These losses are higher at the low-elevation SVr station, and reduced in Mr and BNr stations, respectively. Stable isotopes at Mr suggest that this river is mainly fed by snow melt in spring, with the pulse of water depleted in heavy isotopologues reaching the lower reaches of the river with a delay of about 1–3 months after the onset of melting in March. At SVr, the contribution from tributaries in the low-lying areas, mostly fed by liquid precipitation, dampens the winter signal, so that the recharge of the river is mainly pluvio–nival, compared to Mr which is mostly nivo–pluvial. Bistrița River (at BNr station) has an intermediary type of recharge, with snow contributing more to the discharge in cold winters. A similar distribution of the  $\delta^2\text{H}$  and  $\delta^{18}\text{O}$  values in river water was also observed in the other rivers from higher latitudes, where the snow-melt and elevation effect have a strong influence in the river water isotope variability [15,16,43,44].

#### 4. Conclusions

This study analyzed the stable isotope composition of precipitation and river waters in northeastern part of Romania. The local meteoric water line for the northeastern part of Romania was established as  $\delta^2\text{H} = 7.80 \times \delta^{18}\text{O} + 7.47$ , ( $r^2 = 0.99$ ,  $n = 121$ ), and it is similar to the LMWL of other regions from Romania and the neighboring countries. The variability of  $\delta^{18}\text{O}$  and  $\delta^2\text{H}$  in precipitation is in agreement with the air temperature variability, as shown by the significant correlation coefficient ( $r = 0.77$ ) between the two variables. This indicates that the temperature is the main factor which controls the  $\delta^{18}\text{O}$  variability in precipitation water in this region. The lowest  $\delta^2\text{H}$  and  $\delta^{18}\text{O}$  values generally occur in December, in relation to large-scale atmospheric circulation bringing cold air along north and northeastern trajectories. Superimposed on this general circulation type, Mediterranean cyclones and westerlies bring moisture to the region, with distinct isotopic signatures, that could be useful in reconstructing past circulation changes in the region. The highest  $\delta^2\text{H}$  and  $\delta^{18}\text{O}$  values generally occur in July and August, when high temperatures, related to blocking atmospheric patterns, dominate the area. Low precipitation amounts and dry air favor strong evaporative conditions and associated kinetic fractionation processes in the falling raindrops, leading to distinct patterns of stable isotope of d-excess distribution in rain. Low d-excess values occur in summer and high in autumn and winter, the former related to evaporative processes at the site, and the later to moisture being sourced from high evaporative sites in the neighboring seas (the Mediterranean and the Black Seas). These relationships are further complicated by the local orography, with the Carpathian Mountains acting as an effective barrier against air circulation, thus modulating the effect of atmospheric drivers. These processes are mostly active at the low-elevation stations, with precipitation at high elevations being less influenced.

The stable isotope values in river water suggest that rivers are recharged via subsurface flow, with water from individual rain events being stored in the phreatic zone before recharging the rivers. Winter precipitation is the main contributor in high-mountain area, diminishing towards the low elevation sites, where local rivers contribute water mainly during spring rain events.

Following the analysis of the five case studies, we conclude that the  $\delta^{18}\text{O}$  and d-excess variability are strongly influenced by temperature, presence of snow cover layer and the prevailing large-scale atmospheric circulation. Also, terrestrial geomorphology, which may act as orographic barriers for the prevailing air masses, has a significant influence on the  $\delta^{18}\text{O}$  and d-excess variability. A next logical step would be to extend our analysis to more stations, to have a better spatial overview of the variability of the stable isotopes both in precipitation and river water, as well as to use stable isotopes in groundwater.

**Author Contributions:** V.N.: Conceptualization, writing—original draft; V.N. and C.-A.B.: Formal analysis; V.N., C.-A.B. and M.I.: Writing—review & editing; V.N., C.-A.B. and M.I.: Investigation.

**Funding:** This research was funded by Unitatea Executivă pentru Finanțarea Învățământului Superior, a Cercetării, Dezvoltării și Inovării Romania( UEFISCDI Romania, grants number PN-II-RU-TE-2011-3-0235, PN-III-P1-1.1-TE-2016-2210, 663/2013 and 790/2014), European Economic Area (EEA grants, grant number 18SEE)

and the International Agency for Atomic Energy (IAEA) through the “Application and development of isotope techniques to evaluate human impacts on water balance and nutrient dynamics of large river basins” (grant number RO18452) and “Isotope techniques for the evaluation of water sources in irrigation systems” (grant number 22895) coordinated research programs.

**Acknowledgments:** We thank Aurel Perşoiu for his valuable suggestions and comments and also for providing the financial support both for the collection and analysis of the samples. We thank Aurelia Antonescu, PetruŃ Bistricean, Veronica Ciobanu and Ionel Popa for collecting precipitation and river samples.

**Conflicts of Interest:** The authors declare no conflict of interest. The funders had no role in the design of the study; in the collection, analyses, or interpretation of data; in the writing of the manuscript; or in the decision to publish the results.

## References

1. Bowen, G.J.; Wilkinson, B. Spatial distribution of  $\delta^{18}\text{O}$  in meteoric precipitation. *Geology* **2002**, *30*, 315. [[CrossRef](#)]
2. Dutton, A.; Wilkinson, B.H.; Welker, J.M.; Bowen, G.J.; Lohmann, K.C. Spatial distribution and seasonal variation in  $^{18}\text{O}/^{16}\text{O}$  of modern precipitation and river water across the conterminous USA. *Hydrol. Process.* **2005**, *19*, 4121–4146. [[CrossRef](#)]
3. Hager, B.; Foelsche, U. Stable isotope composition of precipitation in Austria. *Austrian J. Earth Sci.* **2015**, *108*, 2–14. [[CrossRef](#)]
4. Le Duy, N.; Heidbüchel, I.; Meyer, H.; Merz, B.; Apel, H. What controls the stable isotope composition of precipitation in the Mekong Delta? A model-based statistical approach. *Hydrol. Earth Sci.* **2018**, *22*, 1239–1262. [[CrossRef](#)]
5. Sodemann, H.; Schwierz, C.; Vinther, B.M.; Wernli, H.; Masson-Delmotte, V.; Masson-Delmotte, V.; Masson-Delmotte, V. Interannual variability of Greenland winter precipitation sources: 2. Effects of North Atlantic Oscillation variability on stable isotopes in precipitation. *J. Geophys. Res. Biogeosci.* **2008**, *113*, 1–21. [[CrossRef](#)]
6. Gat, J.R. Oxygen and hydrogen isotopes in the hydrologic cycle. *Annu. Earth Planet. Sci.* **1996**, *24*, 225–262. [[CrossRef](#)]
7. Sharp, Z. *Principles of Stable Isotope Geochemistry*, 1st ed.; Rapp, C., Ed.; Pearson Education: Upper Saddle River, NJ, USA, 2007.
8. Ala-Aho, P.; Soulsby, C.; Pokrovsky, O.; Kirpotin, S.; Karlsson, J.; Serikova, S.; Vorobyev, S.; Manasyrov, R.; Loiko, S.; Tetzlaff, D. Using stable isotopes to assess surface water source dynamics and hydrological connectivity in a high-latitude wetland and permafrost influenced landscape. *J. Hydrol.* **2018**, *556*, 279–293. [[CrossRef](#)]
9. Wang, T.; Chen, J.; Li, L. Entropy analysis of stable isotopes in precipitation: Tracing the monsoon systems in China. *Sci. Rep.* **2016**, *6*, 30389. [[CrossRef](#)]
10. Yu, W.; Yao, T.; Tian, L.; Ma, Y.; Kurita, N.; Ichiyanaagi, K.; Wang, Y.; Sun, W. Stable Isotope Variations in Precipitation and Moisture Trajectories on the Western Tibetan Plateau, China. *Arctic, Antarct. Alp.* **2007**, *39*, 688–693. [[CrossRef](#)]
11. Gat, J.R. Environmental Isotopes in the Hydrological Cycle, Principles and Applications (Atmospheric Water). Available online: <http://www.hydrology.nl/ihppublications/149-environmental-isotopes-in-the-hydrological-cycle-principles-and-applications.html> (accessed on 18 October 2018).
12. Sánchez-Murillo, R.; Esquivel-Hernández, G.; Welsh, K.; Brooks, E.S.; Boll, J.; Alfaro-Solís, R.; Valdés-González, J. Spatial and temporal variation of stable isotopes in precipitation across Costa Rica: An analysis of historic GNIP records. *Open J. Hydrol.* **2013**, *3*, 226–240. [[CrossRef](#)]
13. Miljevic, N.R.; Golobocanin, D.D.; Nadeždic, M.L.; Ogrinc, N. Distribution of stable isotopes in the River Sava in Serbia. *Nukleonika* **2008**, *53*, S129–S135.
14. Reckerth, A.; Stichler, W.; Schmidt, A.; Stumpp, C. Long-term data set analysis of stable isotopic composition in German rivers. *J. Hydrol.* **2017**, *552*, 718–731. [[CrossRef](#)]
15. Rank, D.; Wyhlidal, S.; Schott, K.; Weigand, S.; Oblin, A. Temporal and spatial distribution of isotopes in river water in Central Europe: 50 years experience with the Austrian network of isotopes in rivers. *Isot. Environ. Heal. Stud.* **2017**, *54*, 115–136. [[CrossRef](#)]

16. Theakstone, W.H. Oxygen isotopes in glacier-river water, Austre Okstindbreen, Okstindan, Norway. *J. Glaciol.* **2003**, *49*, 282–298. [[CrossRef](#)]
17. Ogrinc, N.; Kanduč, T.; Stichler, W.; Vreca, P. Spatial and seasonal variations in  $\delta^{18}\text{O}$  and  $\delta\text{D}$  values in the River Sava in Slovenia. *J. Hydrol.* **2008**, *359*, 303–312. [[CrossRef](#)]
18. Kang, S.; Kreutz, K.J.; Mayewski, P.A.; Qin, D.; Yao, T. Stable-isotopic composition of precipitation over the northern slope of the central Himalaya. *J. Glaciol.* **2002**, *48*, 519–526. [[CrossRef](#)]
19. Baisden, W.T.; Keller, E.D.; Van Hale, R.; Frew, R.D.; Wassenaar, L.I. Precipitation isoscapes for New Zealand: enhanced temporal detail using precipitation-weighted daily climatology. *Isot. Environ. Heal. Stud.* **2016**, *52*, 1–10. [[CrossRef](#)] [[PubMed](#)]
20. Liu, J.; Fu, G.; Song, X.; Charles, S.P.; Zhang, Y.; Han, D.; Wang, S. Stable isotopic compositions in Australian precipitation. *J. Geophys. Res. Biogeosci.* **2010**, *115*, 1–16. [[CrossRef](#)]
21. Sandu, I.; Pescaru, V.I.; Poiana, I. *Clima Romaniei; Editura Academiei Române: București (in Romanian); Romanian Academy: Bucharest, Romania, 2008; ISBN 973-27-1674-8.*
22. Cornes, R.C.; Van Der Schrier, G.; Besselaar, E.J.M.V.D.; Jones, P.D. An Ensemble Version of the E-OBS Temperature and Precipitation Data Sets. *J. Geophys. Res. Atmos.* **2018**, *123*, 9391–9409. [[CrossRef](#)]
23. Bădăluță, C.-A.; Perșoiu, A.; Ionita, M.; Nagavciuc, V.; Bistricean, P.-I. Stable H and O isotope-based investigation of moisture sources and their role in river and groundwater recharge in the NE Carpathian Mountains, East-Central Europe. *Isot. Environ. Heal. Stud.* **2019**, *55*, 161–178. [[CrossRef](#)]
24. Dansgaard, W. Stable isotopes in precipitation. *Tellus* **1964**, *4*, 436–468.
25. Pfahl, S.; Sodemann, H. What controls deuterium excess in global precipitation? *Clim. Past* **2014**, *10*, 771–781. [[CrossRef](#)]
26. Kalnay, E.; Kanamitsu, M.; Kistler, R.; Collins, R.; Deavean, D.; Gandin, L.; Iredell, M.; Saha, S.; White, G.; Woollen, J.; et al. NCAR 40-year reanalysis project. *Bull. Am. Meteor. Soc.* **1996**, *77*, 437–470. [[CrossRef](#)]
27. Hall, D.K.; Riggs, G.A. *MODIS/Terra Snow Cover Monthly L3 Global 0.05Deg CMG; Version 6; NASA National Snow and Ice Data Center Distributed Active Archive Center: Boulder, Co, USA.*
28. Holko, L.; Dóša, M.; Michalko, J.; Kostka, Z.; Šanda, M. Isotopes of oxygen-18 and Deuterium in precipitation in Slovakia. *J. Hydrol. Hydromech.* **2012**, *60*, 265–276. [[CrossRef](#)]
29. Christner, E.; Aemisegger, F.; Pfahl, S.; Werner, M.; Cauquoin, A.; Schneider, M.; Hase, F.; Barthlott, S.; Schädler, G. The climatological impacts of continental surface evaporation, rainout, and subcloud processes on  $\delta\text{D}$  of water vapor and precipitation in Europe. *J. Geophys. Res. Atmos.* **2018**, *123*, 4390–4409. [[CrossRef](#)]
30. Bojar, A.V.; Halas, S.; Bojar, H.P.; Chmiel, S. Stable isotope hydrology of precipitation and groundwater of a region with high continentality, South Carpathians, Romania. *Carpath. J. Earth Environ. Sci.* **2017**, *12*, 513–524. [[CrossRef](#)]
31. Hussain, S.; Xianfang, S.; Jianrong, L.; Mei, H.D.; Hu, Y.L.; Huang, W. Controlling factors of the stable isotope composition in the precipitation of Islamabad, Pakistan. *Adv. Meteorol.* **2015**, *2015*, 1–11. [[CrossRef](#)]
32. Tappa, D.J.; Kohn, M.J.; McNamara, J.P.; Benner, S.G.; Flores, A.N. Isotopic composition of precipitation in a topographically steep, seasonally snow-dominated watershed and implications of variations from the global meteoric water line. *Hydrol. Process.* **2016**, *30*, 4582–4592. [[CrossRef](#)]
33. Ersek, V.; Onac, B.P.; Perșoiu, A. Kinetic processes and stable isotopes in cave dripwaters as indicators of winter severity. *Hydrol. Process.* **2018**, *32*, 2856–2862. [[CrossRef](#)]
34. Kern, Z.; Fórizs, I.; Perșoiu, A.; Nagy, B. Stable isotope study of water sources and of an ice core from the Borțig Ice Cave, Romania. *Data Glaciol. Stud.* **2009**, *107*, 175–182.
35. Perșoiu, A.; Bojar, A.-V.; Onac, B.P. Stable isotopes in cave ice: what do they tell us? *Studia UBB Geol.* **2007**, *52*, 59–62.
36. Vodila, G.; Palcsu, L.; Futó, I.; Szántó, Z. A 9-year record of stable isotope ratios of precipitation in Eastern Hungary: Implications on isotope hydrology and regional palaeoclimatology. *J. Hydrol.* **2011**, *400*, 144–153. [[CrossRef](#)]
37. Gat, J.R.; Mook, W.G.; Meijer, H.A.J. *Environmental Isotopes in the Hydrological Cycle: Atmospheric Water; IHP-V, Technical Documents in Hydrology; UNESCO: Paris, France, 2001.*
38. Campins, J.; Genovés, A.; Picornell, M.A.; Jansà, A. Climatology of Mediterranean cyclones using the ERA-40 dataset. *Int. J. Climatol.* **2011**, *31*, 1596–1614. [[CrossRef](#)]

39. Gat, J.R.; Klein, B.; Kushnir, Y.; Roether, W.; Wernli, H.; Yam, R.; Shemesh, A. Isotope composition of air moisture over the Mediterranean Sea: An index of the air-sea interaction pattern. *Tellus B: Chem. Phys. Meteorol.* **2003**, *55*, 953–965. [[CrossRef](#)]
40. IAEA *Isotopic Composition Of Precipitation in the Mediterranean Basin in Relation to Air Circulation Patterns and Climate*; Final report of a coordinated research project 2000–2004, Isotope Hydrology Section; International Atomic Energy Agency: Vienna, Austria, 2005.
41. Drăgușin, V.; Balan, S.; Blamart, D.; Forray, F.L.; Marin, C.; Mirea, I.; Nagavciuc, V.; Perșoiu, A.; Tîrlă, L.; Tudorache, A.; et al. Transfer of environmental signals from surface to the underground at Ascunsă Cave, Romania. *Hydrol. Earth Sci. Discuss.* **2017**, *21*, 1–23.
42. Vystavna, Y.; Diadin, D.; Huneau, F. Defining a stable water isotope framework for isotope hydrology application in a large trans-boundary watershed (Russian Federation/Ukraine). *Isot. Environ. Health Stud.* **2018**, *54*, 147–167. [[CrossRef](#)] [[PubMed](#)]
43. Halder, J.; Terzer, S.; Wassenaar, L.I.; Araguas-Araguas, L.J.; Aggarwal, P.K. The Global Network of Isotopes in Rivers (GNIR): integration of water isotopes in watershed observation and riverine research. *Hydrol. Earth Sci.* **2015**, *19*, 3419–3431. [[CrossRef](#)]
44. Ogrinc, N.; Kocman, D.; Miljević, N.; Vreča, P.; Vrzel, J.; Povinec, P. Distribution of H and O stable isotopes in the surface waters of the Sava River, the major tributary of the Danube River. *J. Hydrol.* **2018**, *565*, 365–373. [[CrossRef](#)]



© 2019 by the authors. Licensee MDPI, Basel, Switzerland. This article is an open access article distributed under the terms and conditions of the Creative Commons Attribution (CC BY) license (<http://creativecommons.org/licenses/by/4.0/>).